In Silico Pharmacology (2025) 13:29
https://doi.org/10.1007/s40203-025-00320-w

ORIGINAL RESEARCH

De novo in silico screening of natural products for antidiabetic drug discovery: ADMET profiling, molecular docking, and molecular dynamics simulations

Sulyman Olalekan Ibrahim[1] · Yusuf Oloruntoyin Ayipo[2,3] · Halimat Yusuf Lukman[4] · Fatimah Aluko Abubakar[5] · Asiat Na'Allah[6] · Rashidat Arije Katibi-Abdullahi[3] · Marili Funmilayo Zubair[1] · Olubunmi Atolani[7]

Received: 31 December 2024 / Accepted: 7 February 2025
© The Author(s), under exclusive licence to Springer-Verlag GmbH Germany, part of Springer Nature 2025

Abstract

Epigenetic dysfunction which has implicated disease conditions such as diabetes highlights the urgency for the discovery of novel therapeutic alternatives. The rising global incidences of diabetes and the limitations of existing treatments further exacerbate the quest for novel antidiabetic agents' discovery. This study leverages computational approaches to screen selected bioactive natural product phytoconstituents for their potential anti-diabetic properties. Utilizing pharmaceutical profiling, ADMET (Absorption, Distribution, Metabolism, Excretion, and Toxicity) predictions, molecular docking, and molecular dynamics (MD) simulations, the drug-likeness and binding affinity of these natural compounds against human pancreatic amylase was investigated. Out of the total 24,316 ZINC compounds screened for their binding scores with amylase, ZINC85593620, ZINC85593668, and ZINC85490447 came top. The compounds had higher binding scores than the standards (acarbose and ranirestat) with ZINC85593620 having the highest docking score of − 12.162 kcal/mol and interacted with key amino acid residues such as TRP 59, ILE 148, and ASP 197. Further validation through MD simulations reveals that all the compounds showed minimal fluctuations relative to the standards indicating strong and stable binding interactions suggesting potential effective inhibition of the enzyme. ZINC85593620 and ZINC85593668 showed promising distribution and availability characteristics for amylase inhibition. Overall, the compounds displayed potential amylase inhibition which underscores their use as promising natural products in developing new antidiabetic drugs. Further experimental validations are recommended to offer a potential solution to the pressing need for safer and more effective antidiabetic therapies.

Keywords Natural products · Molecular docking · Molecular dynamics simulations · ADMET profiling · Antidiabetic

✉ Sulyman Olalekan Ibrahim
ibrahim.sio@unilorin.edu.ng

[1] Department of Industrial Chemistry, Faculty of Physical Sciences, University of Ilorin, Ilorin, Nigeria

[2] Centre for Drug Research, Universiti Sains Malaysia, USM, George Town, Pulau Pinang, Malaysia

[3] Department of Chemistry and Industrial Chemistry, Faculty of Pure and Applied Sciences, Kwara State University, Malete, Ilorin, Nigeria

[4] Department of Chemical Sciences, College of Natural and Applied Sciences, Summit University, Offa, Nigeria

[5] Department of Biochemistry, Faculty of Life Sciences, University of Ilorin, Ilorin, Nigeria

[6] Department of Biochemistry, Faculty of Pure and Applied Sciences, Kwara State University, Malete, Ilorin, Nigeria

[7] Department of Chemistry, Faculty of Physical Sciences, University of Ilorin, Ilorin, Nigeria

Published online: 17 February 2025

Introduction

Diabetes mellitus is a chronic metabolic disorder characterized by hyperglycemia resulting from insulin dysfunction. The prevalence of diabetes is escalating at an alarming rate globally, imposing a significant burden on healthcare systems, economies, and societies (Lu et al. 2024; Asogwa et al. 2023; Hossain et al. 2024). According to the International Diabetes Federation (IDF), approximately 463 million adults were living with diabetes in 2019, and this number is projected to rise to 700 million by 2045. The disease is associated with a myriad of complications, including cardiovascular diseases, nephropathy, neuropathy, retinopathy, and increased susceptibility to infections, which collectively contribute to elevated morbidity and mortality (Sun et al. 2022; Teo et al. 2021).

Despite the availability of various antidiabetic agents, including insulin and oral hypoglycemic drugs, the management of diabetes remains suboptimal for many patients. Current therapies often fail to achieve and maintain glycemic control, and they are frequently associated with adverse effects such as hypoglycemia, weight gain, gastrointestinal disturbances, and cardiovascular risks (Edache et al. 2021; AbdulRasheed-Adeleke et al. 2023). Moreover, the progressive nature of diabetes necessitates combination therapies which often leads to treatment failures over time. Therefore, there is a pressing need to explore and develop novel antidiabetic drugs with improved efficacy, safety profiles, and mechanisms of action (Yan et al. 2024; Koufakis et al. 2020).

The global burden of diabetes is immense, with substantial implications for healthcare costs, productivity, and quality of life. Direct medical costs for diabetes management include expenses related to medications, monitoring devices, healthcare services, and treatment of complications. Indirect costs arise from lost productivity, absenteeism, disability, and premature mortality (Mahapatra et al. 2022).

Current antidiabetic therapies encompass a range of pharmacological classes, each targeting different aspects of glucose homeostasis. These include insulin, which is essential for patients with type 1 diabetes and advanced type 2 diabetes; sulfonylureas and meglitinides, which stimulate insulin secretion; biguanides such as metformin, which reduce hepatic glucose production; thiazolidinediones, which enhance insulin sensitivity; alpha-glucosidase inhibitors, which delay carbohydrate absorption; and incretin-based therapies, which enhance incretin hormone activity (Weinberg Sibony et al. 2023; Olanrewaju et al. 2023). However, each of these therapies has limitations that impede optimal diabetes management.

Insulin therapy, while effective and life-saving, it requires cautious and continuous observation to avoid hypoglycemia and is associated with weight gain and injection site complications (Mansuri et al. 2024). Oral hypoglycemic agents such as sulfonylureas and meglitinides carry a risk of hypoglycemia and can lose efficacy over time. Metformin, the first-line therapy for type 2 diabetes, is contraindicated in patients with renal impairment and can cause gastrointestinal side effects (Houglum et al. 2024; Stoica et al. 2019). Thiazolidinediones are linked to weight gain, fluid retention, and an increased risk of heart failure. Alpha-glucosidase inhibitors often cause gastrointestinal disturbances, limiting their use (Arun and Vettath 2024). Incretin-based therapies, including GLP-1 receptor agonists and DPP-4 inhibitors, offer advantages such as weight loss and low hypoglycemia risk but have also been associated with pancreatitis and other adverse effects in some cases (Zhang et al. 2017). Existing alpha-amylase and glucosidase inhibitors have been reported to induce side effects such as hypoglycemia, diarrhea, flatulence, and bowel bloating (Khursheed et al. 2019).

Given these limitations, there is a critical need for new antidiabetic drugs that can address the unmet needs of diabetes management. Such drugs should ideally offer superior glycemic control, minimal adverse effects, and novel mechanisms of action that complement existing therapies. Drug banks present an attractive avenue for discovering such candidates, as they provide access to a vast array of compounds with known safety profiles and biological activities (Prajapati et al. 2024).

One promising approach to addressing this need is using drug banks, which are repositories of compounds previously identified and characterized, including approved drugs, investigational drugs, and bioactive molecules. Drug banks are comprehensive repositories that store various compounds, including FDA-approved drugs, investigational new drugs (INDs), and other bioactive molecules. These compounds have undergone varying degrees of characterization, including preclinical and clinical evaluations, making them valuable resources for drug discovery and repurposing efforts. Drug repurposing involves identifying new therapeutic targets for existing drugs, which can significantly shorten the drug development timeline and reduce costs compared to traditional drug discovery routes.

Recent advances in computational biology, bioinformatics, and high-throughput screening have further enhanced the feasibility of drug repurposing. In silico approaches, such as molecular docking, virtual screening, and network pharmacology, enable the identification of potential drug-target interactions and biological pathways relevant to diabetes. These methods, combined with experimental validation, can rapidly identify promising candidates from drug

banks for further development as antidiabetic agents (Hernandez et al. 2019; Ahmed et al. 2023; Ibrahim et al. 2024a). Hence, this study aimed at identifying druggable and viable amylase inhibitors from natural products' phytochemical drug banks as potential antidiabetic compounds.

Methods

Ligand selection and preparation

Twenty-four thousand, three hundred and sixteen (24,316) compounds (SDF format) were retrieved from the natural compounds repository of Traditional Chinese Medicine (TCM) database@Taiwan (Lv et al. 2023; Wang et al. 2024) (https://zinc12.docking.org/browse/catalogs/natural-products) (Accessed on 13 September 2024). The 3D structure of the standard reference drugs; ranirestat and acarbose were obtained from PubChem database (https://pubchem.ncbi.nlm.nih.gov/). Using LigPrep wizard (LigPrep, Schrodinger, LCC, New York, NY, 2019) of the Maestro 12.8 suites, the ligands were prepared by adding proton, energy minimizing protonation, geometry estimation, and partial atomic charges using OPLS-3e force field (Ayipo et al. 2021; Jangid et al. 2024). The prepped ligands were then saved in a LigPrep output folder.

Protein selection and preparation

The PDB format of the human pancreatic amylase (PDB: 4W93) was downloaded from the protein data bank (www.rscb.org/) (Accessed on 14 September 2024). The human pancreatic amylase was preprocessed according to the methods described by Ayipo and his coworkers (Ayipo et al. 2022) by using the protein preparation wizard of the Maestro 12.8 suite to assign bond order, protonation, fill missing loops, optimize and minimize energy with the OPLS-3e force field. The best druggable binding site and ready-to-dock grid box were selected based on the active pocket of the co-ligand.

Molecular docking

The study used Maestro 12.8 Glide's HTVS, SP, and XP molecular docking modules to screen receptor grid and ligand output files. The top three compounds with good scoring functions, binding interactions affinity, and MMGBSA binding energy values were selected for further investigation. The docking techniques were validated using standard inhibitors (acarbose and ranirestat) and co-crystallized ligands. The top compounds were then subjected to molecular dynamics (MD) simulations for their binding interaction and stability.

Molecular dynamics simulation

The MD simulation of the top docked complexes was carried out using the Desmond package (Desmond 2020–3, Schrodinger LLC) (Schrodinger Release 2020–3, 2021) in a solvent-soaked orthorhombic periodic box, with the system charges neutralized with $Na+$ and $Cl-$ counter ions. The solvated system was minimized and relaxed using OPLS-3e force field parameters. The simulation was carried out for 100 ns, and trajectory snapshots were recorded at an interval of 100 ps. The MD trajectories were analyzed using Desmond's simulation interaction diagram to predict the binding orientation of the ligand to the enzyme (Khan et al. 2024; Osmaniye et al. 2022; Schönherr et al. 2024). The parameters observed from the MD trajectories were protein/ligand root mean square deviation (RMSD), protein C–α atoms root mean square fluctuation (RMSF), the radius of gyration (Rg), and Molecular/Mechanics Generalized Born Surface Area (MM-GBSA) binding free energy analysis.

Binding free energy calculations

The binding free energies of the selected ligand–protein complexes were calculated using the MM-GBSA approach employing the Python script (thermal_mmgbsa.py). The prime MMGBSA binding free energy for assessed from 0 to 1000 frames, having a 10 steps sampling size in the simulation trajectory with the Variable Dielectric Surface Generalized Born (VSGB) solvation model associated with the OPLS-3e force field. The overall ligand–protein complexes MM-GBSA-based binding free energy (ΔG_{Bind}) was calculated using the equation given below

$$\Delta G_{bind} = E_{complex\ (minimized)} - \left(E_{Ligand\ (minimized)} + E_{protein\ (minimized)}\right)$$

Pharmacokinetics and pharmacodynamics predictions

The physicochemical and pharmacokinetics properties which define the absorption, distribution, metabolism, excretion, and toxicity (ADMET) profiles of the selected ligands and reference drugs were estimated using the pkCSM pharmacokinetics predictor https://biosig.lab.uq.edu.au/pkcsm/ by the input of SMILE files. Similarities and closeness of the top compounds to reference drug compounds were generally used as benchmarks for the druggability of the ligands.

Table 1 Docking scores of Top Three compounds, Co-ligand, and Control drugs

Compound ID	Docking scores (kcal/mol)			Interacted Amino acid residue	MMGBSA (Δ_{Gbind}) (Kcal/mol)
	XP	SP	HTVS		
ZINC85593620	−12.162	−9.429	−7.797	TRP 59, ILE 148, THR 163, ARG 195, ASP 197, LYS 200, GLU233, ASP 298	−38.14
ZINC85593668	−11.629	−9.874	-8.097	ASP 197, GLU 233, GLU 240, ASP 300	−42.29
ZINC85490447	−11.201	−9.525	−7.768	THR 163, HIE 201, GLU 233, ASP 300, HIP 305, ASP 356	−56.62
4W93– Co-ligand	−11.536	−8.862	−7.801	TRP 59, GLN 63, LYS 200, GLU 233, GLU 240, ASP 300	−62.04
Acarbose	−12.138	−6.402	−4.394	HIE 201, GLU 233, ILE 235, ASP 300	−59.25
Ranirestat	−6.185	−5.489	−4.497	TRP 59, ARG 195, GLU 233, HIP 305	−45.07

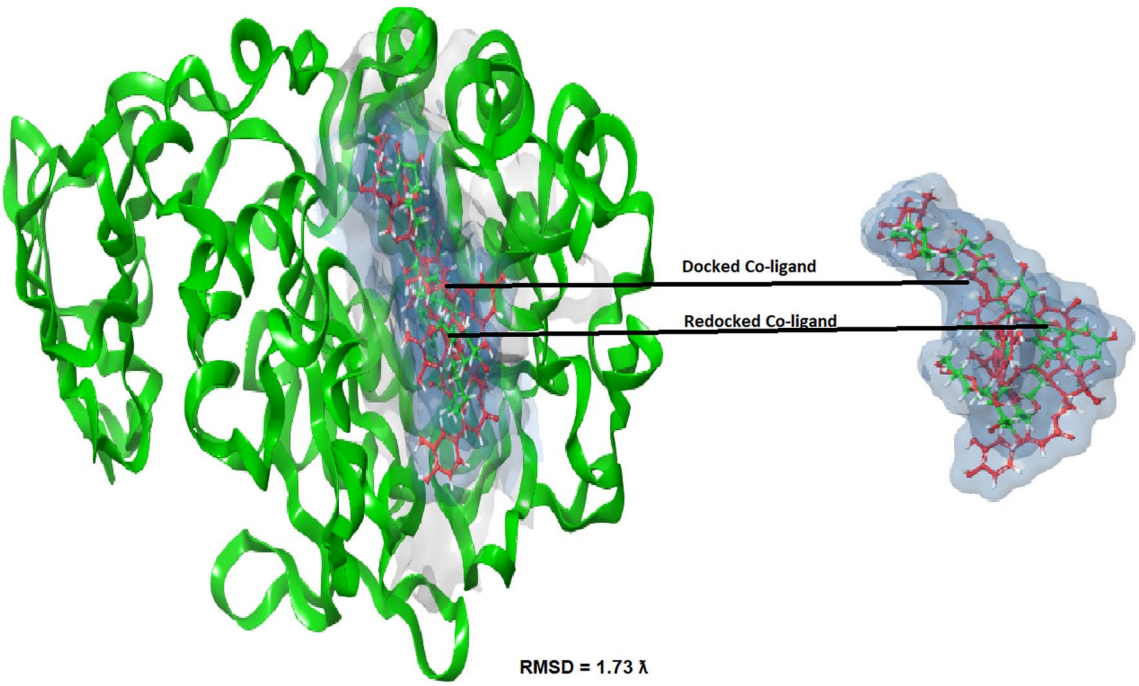


Fig. 1 Superimposed structures of co-crystallized and re-docked reference ligands at the active pocket of residues of human pancreatic amylase. Red: co-crystallized, Green: redocked

Results

The binding scores of the top three ZINC compounds (ZINC85593620, ZINC85593668, and ZINC85490447) with human pancreatic amylase are presented in Table 1. In XP mode, ZINC85593620 exhibited the highest docking score of−12.162 kcal/mol and interacted with multiple key residues such as TRP 59, ILE 148, and ASP 197. The MMGBSA binding energy of−38.14 kcal/mol further supports its potential as an effective inhibitor. ZINC85593668 had a docking score of−11.629 kcal/mol in XP mode, interacted with residues including ASP 197 and GLU 240 residues of the target with a binding energy of−42.29 kcal/mol (Table 1). In XP mode, ZINC85490447 demonstrates a docking score of−11.201 kcal/mol interacted with residues like THR 163 and GLU 233 with binding energy of−56.62 kcal/mol (Table 1). While acarbose had a docking score of−12.138 kcal/mol, interacted with residues such as GLU 233 and ASP 300, with a binding energy of−59.25 kcal/mol (Table 1), ranirestat presented the highest docking score of−6.185 kcal/mol and interacted with TRP 59 and GLU 233 residues of the target. Ranirestat complex displayed a binding energy of −45.07 kcal/mol (Table 1).

The docking was validated by superimposing the structures of co-crystallized and re-docked reference ligands within the active site of the target (Fig. 1). Figures 2, 3, 4, 5 and 6 presented the ligand interactions with key amino acid residues within the enzyme's active site. Acarbose interacted with the active site, maintaining proximity to critical residues and hydrogen bonds interaction with GLU 233 and ASP 300 and hydrophobic interactions with TRP 59 and ILE 148

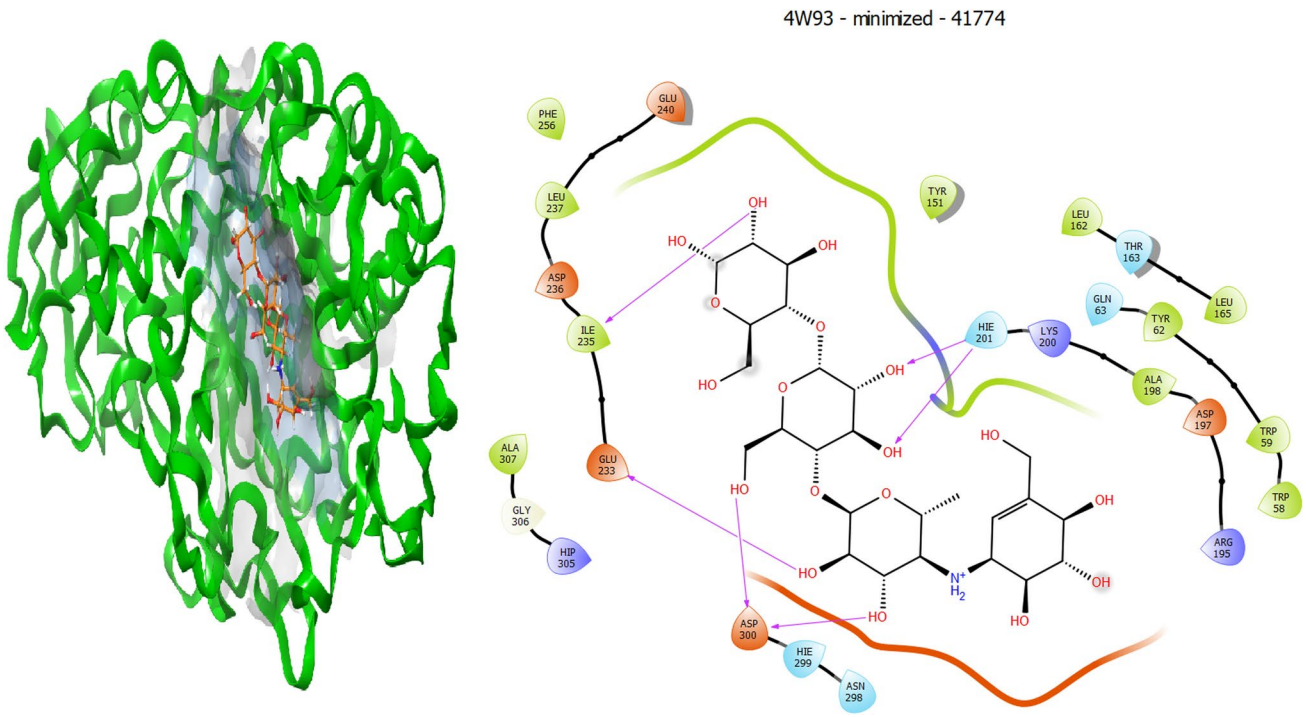


Fig. 2 2D and 3D Binding poses of the interaction of acarbose with amino acid residues of human pancreatic amylase

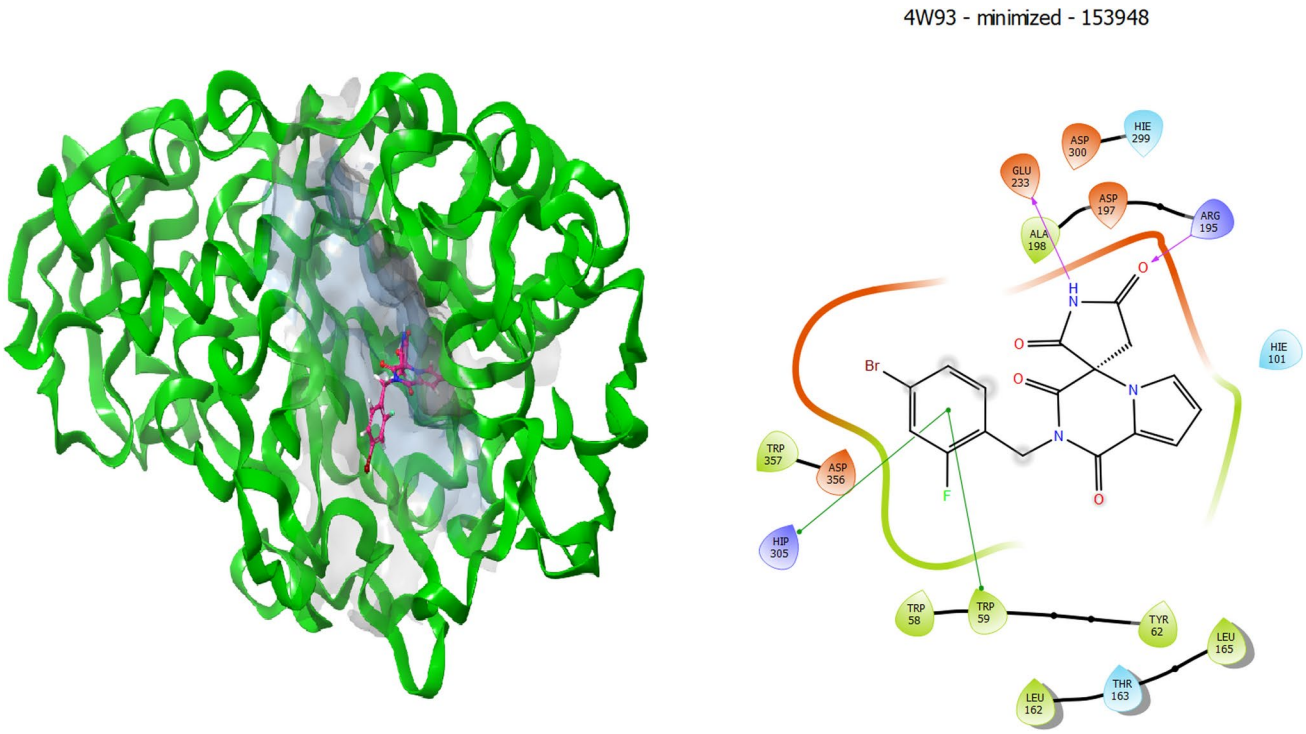


Fig. 3 2D and 3D Binding poses of the interaction of ranirestat with amino acid residues of Human pancreatic amylase

(Fig. 2). Ranirestat interacted in hydrogen bonds with GLU 233 and HIP 305 of the enzyme, along with some hydrophobic contacts (Fig. 3). The Co-crystallized ligand fits well within the binding pocket, and displayed crucial hydrogen bonds with residues such as GLU 233 and GLU 240, confirming the reliability of the docking protocol (Fig. 4). For the compounds, ZINC85490447 maintained a stable conformation in the enzyme's active site and shows hydrogen

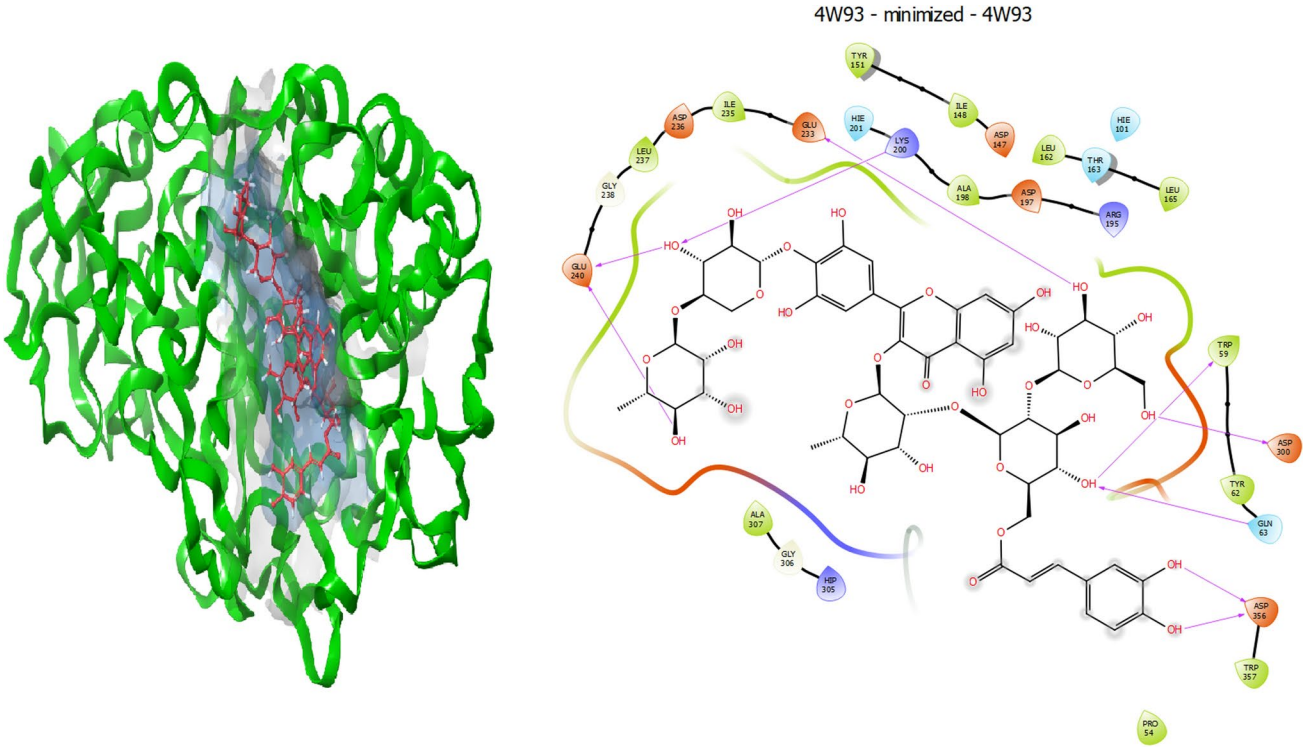


Fig. 4 2D and 3D Binding poses of the interaction of Co-crystallized ligand with amino acid residues of human pancreatic amylase

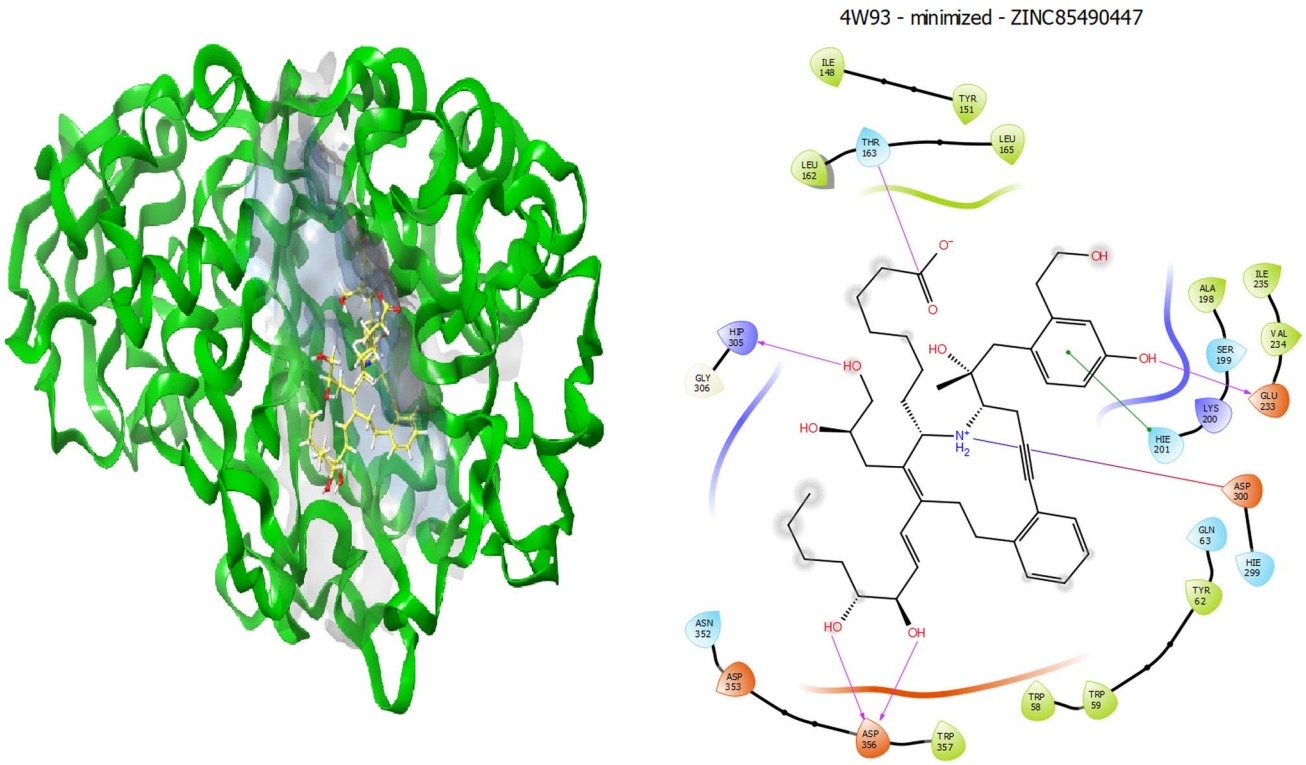


Fig. 5 2D and 3D Binding poses of the interaction of ZINC85490447 with amino acid residues of Human pancreatic amylase

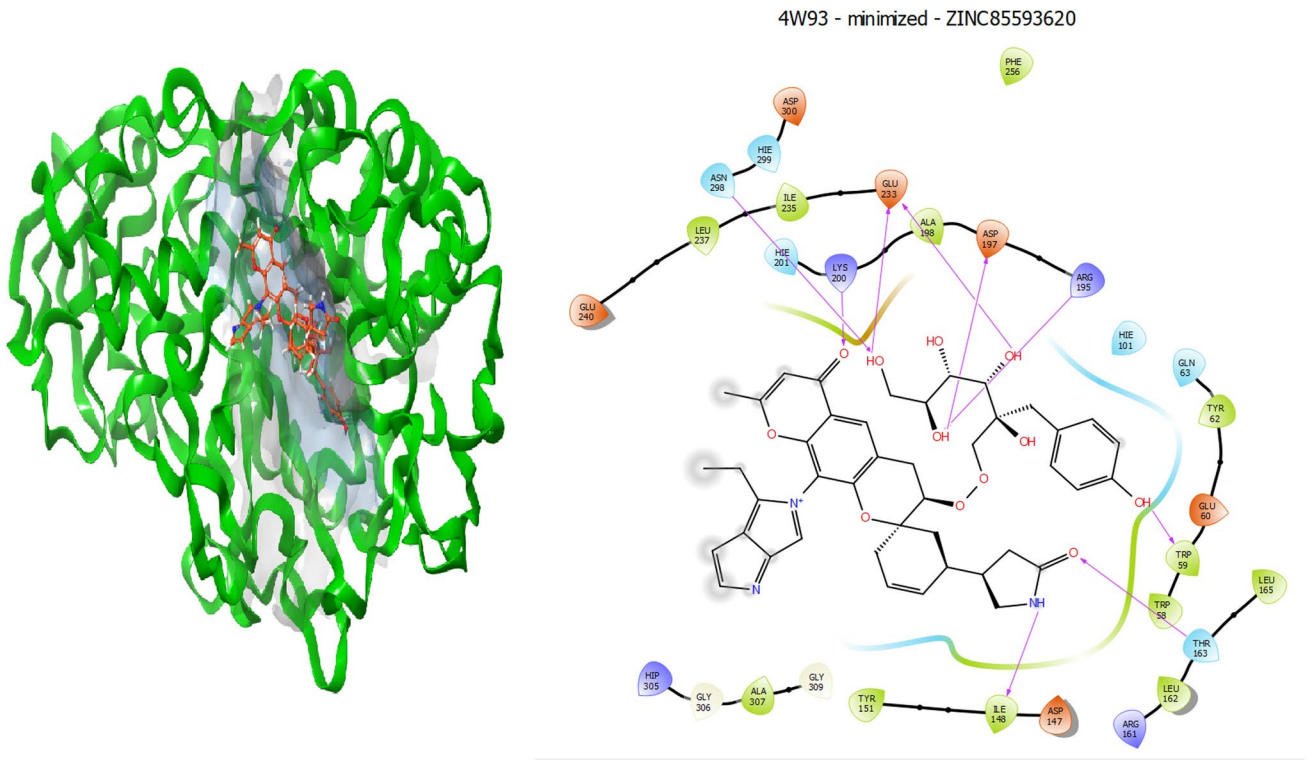


Fig. 6 2D and 3D Binding poses of the interaction of ZINC85593620 with amino acid residues of human pancreatic amylase

bonds with THR 163, HIE 201, and ASP 300 (Fig. 5). While ZINC85593620 interacted in hydrogen bonds with TRP 59, ILE 148, and ASP 197 (Fig. 6), ZINC85593668 made significant hydrogen bonds with ASP 197 and GLU 240 and some hydrophobic interactions (Fig. 7).

The apo-enzyme demonstrated minor fluctuations initially, stabilizing around 2 Å while ranirestat complex showed consistent stability around 2.5 Å throughout the simulation, with slight fluctuations. A stable RMSD pattern was observed in the acarbose-enzyme complex at around 2.2 Å, with minimal deviations. However, the co-ligand complex had higher initial fluctuations, settling around 2.8 Å. ZINC85490447 demonstrated moderate fluctuations with an RMSD stabilizing around 2.5 Å, ZINC85593620 RMSD values remain stable around 2 Å, and ZINC85593668 stabilizes around 2.3 Å (Fig. 8). Figure 9 shows the RMSF-Protein Cα atoms plots of amino acid residues in human pancreatic amylase. Ligands such as ZINC85593668 and ZINC85593620 exhibited low RMSF values throughout the simulation.

Figures 10, 11, 12, 13, 14 and 15 illustrates the interactive contacts between the ZINC compounds, co-ligand, and control drugs with human pancreatic amylase enzyme. The bar charts display the distribution of four types of interactions: hydrogen bonds (H-bonds, green), hydrophobic interactions (purple), ionic interactions (red), and water bridges (blue). These interactions are critical for the stability and efficacy of the ligand binding within the enzyme's active site. ZINC85593620 shows significant hydrogen bonding and hydrophobic interactions with residues such as TRP 59, ILE 148, and THR 163. Similarly, ZINC85593668, presented hydrogen bonding and hydrophobic interactions, particularly with residues ASP 197 and GLU 240. The co-ligand showed a balanced distribution of hydrogen bonds, hydrophobic interactions, ionic interactions, and water bridges with residues such as TRP 59 and GLU 233. ZINC85490447 shows significant hydrogen bonding and hydrophobic interactions with residues THR 163 and HIE 201. Acarbose formed hydrogen bonds with GLU 233 and ASP 300 while ranirestat formed hydrogen bonds and hydrophobic interactions, particularly with residues TRP 59 and GLU 233.

Figure 16 illustrates the radius of gyration for the Human pancreatic amylase enzyme in complex with different selected ligands, control drug (Ranirestat and Metformin), and the co-crystallized ligands over a 100-ns (ns) simulation period. The rGyr of ranirestat and acarbose complex fluctuated around a consistent average. ZINC85490447 exhibited moderate fluctuations, ZINC85593620 complex demonstrated stable fluctuations with consistent rGyr values, and ZINC85593668 complex also maintained stable fluctuations with minimal fluctuations (Fig. 16).

The ADMET properties of the compounds and standard reference drugs are presented on Table 2. Compounds

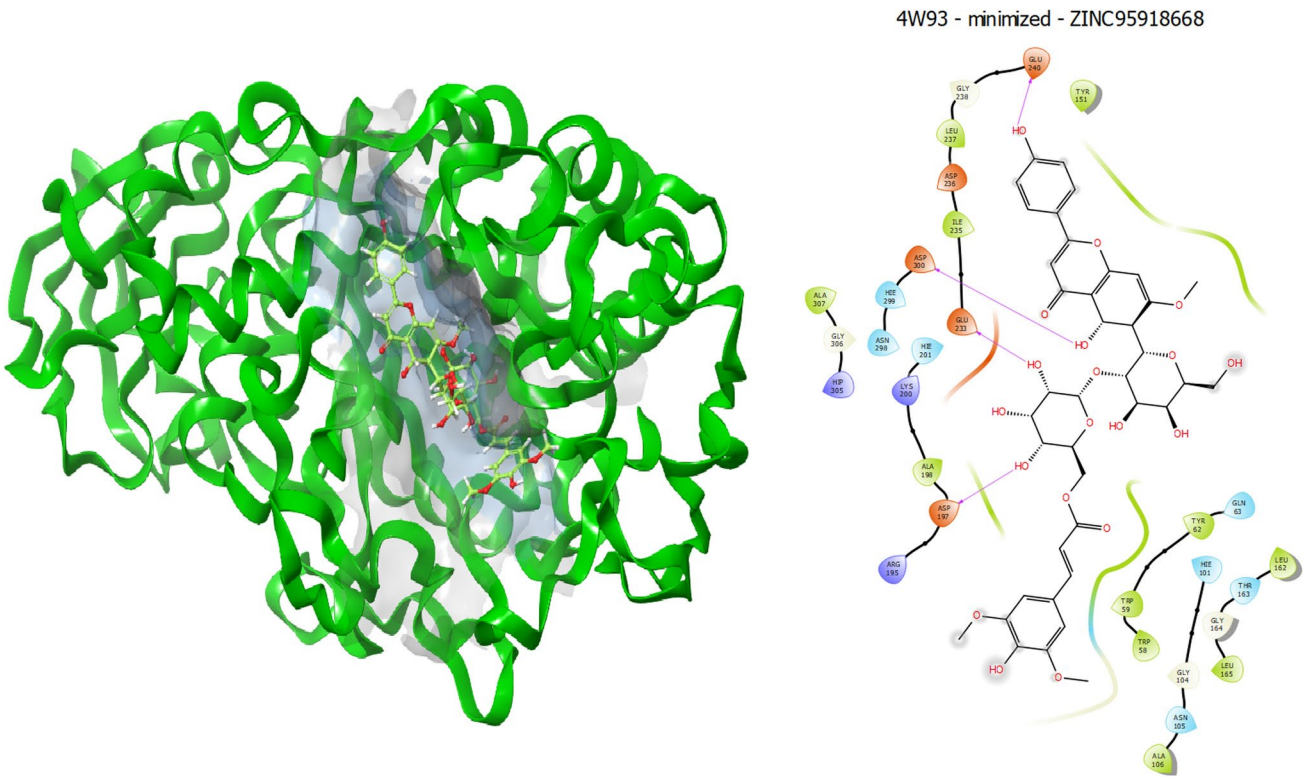


Fig. 7 2D and 3D Binding poses of the interaction of ZINC85593620 with amino acid residues of human pancreatic amylase

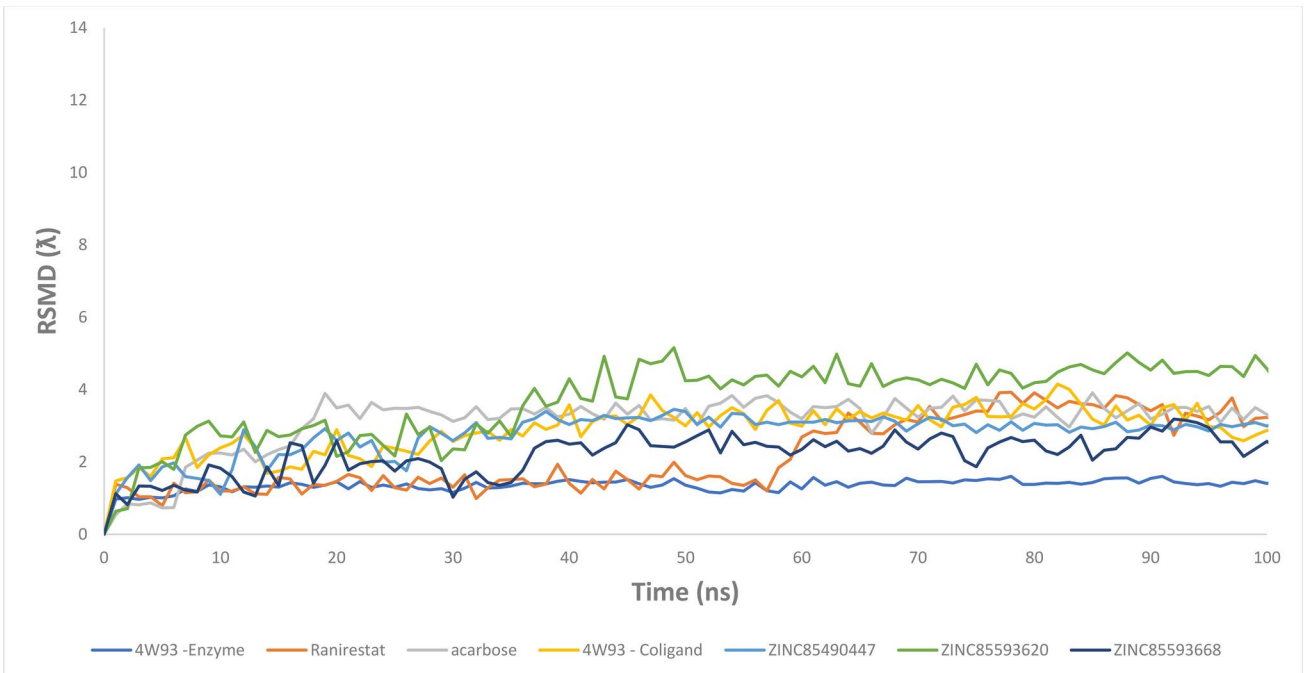


Fig. 8 Time-dependent RMSD during 100 ns MD simulations of human pancreatic amylase enzyme backbone with top ZINC compounds and reference drugs (acarbose and ranirestat). The human pancreatic *amylase* enzyme backbone attained and maintained equilibrium throughout simulation time of 100 ns, indicating good stability with an average fluctuation of 1.5 Å throughout the simulation period. All the selected ligands including the co-ligand and control drugs showed good contact with the protein backbone throughout the 100 ns simulation maintaining a good stability with an average fluctuation of < 2.0 Å throughout the simulation, indicating better stability as shown in Fig. 3 above

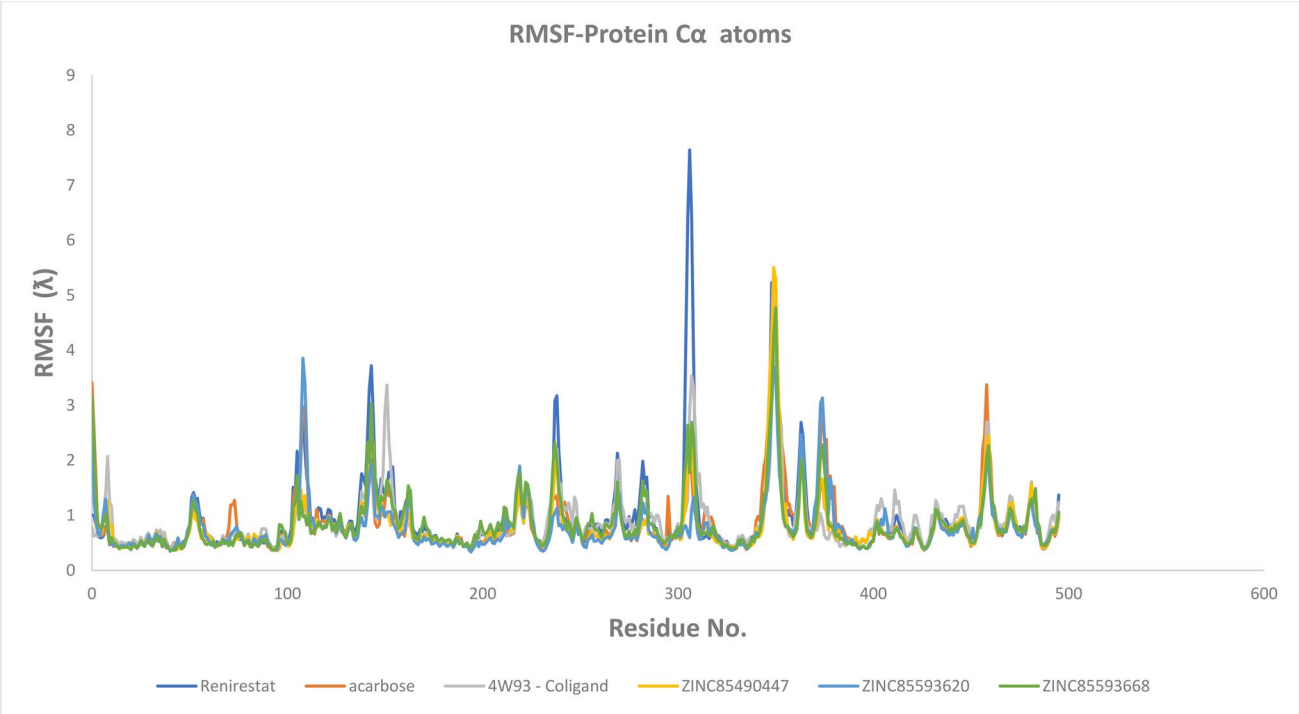


Fig. 9 RMSF plot of human pancreatic amylase enzyme backbone with top ZINC compounds and reference drugs (acarbose and ranirestat)

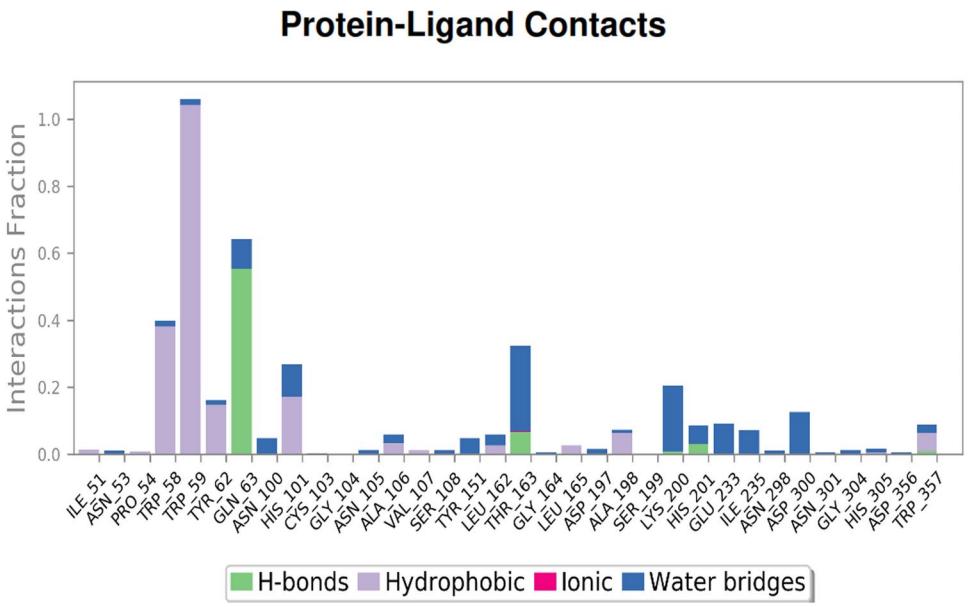


Fig. 10 Bar charts indicating the interactive contacts between ranirestat and the amino acid residues of human pancreatic amylase

ZINC85593620 and ZINC85593668 exhibited lower solubility, negative permeability values relative to acarbose with high water solubility of − 1.482 log mol/L (Table 2). Ranirestat had positive Caco2 permeability (1.288 log Papp in 10^{-6} cm/s) while the natural compounds demonstrated negative Caco2 permeability ZINC85593620 but with substantial absorption (58.339%). However, acarbose and the co-ligand possessed low absorption rates (Table 2). All compounds exhibit low skin permeability (log Kp around − 2.735). While the natural compounds are substrates of P-glycoprotein, they are non-inhibitors of P-glycoprotein I inhibitors, however, ZINC85490447 is the only inhibitor of P-glycoprotein II inhibitor (Table 2). ZINC85593620 and ZINC85593668 exhibit positive Volume of Distribution (VDss) values relative to acarbose and the co-crystallized ligand that have negative VDss values. In addition, ZINC85593620 and ZINC85593668 exhibited appreciable unbound fractions, were non-substract for renal

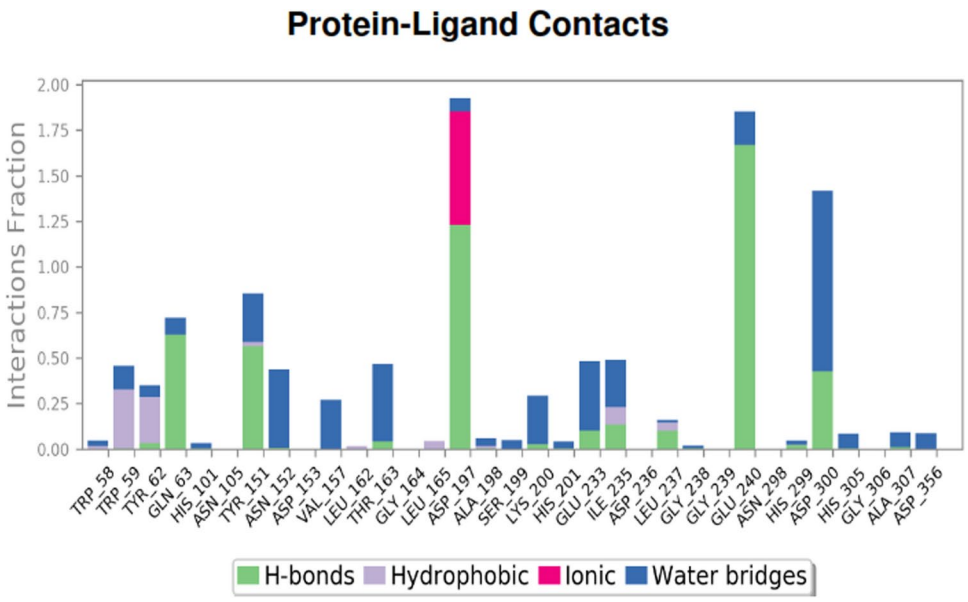


Fig. 11 Bar charts indicating the interactive contacts between acarbose and the amino acid residues of human pancreatic amylase

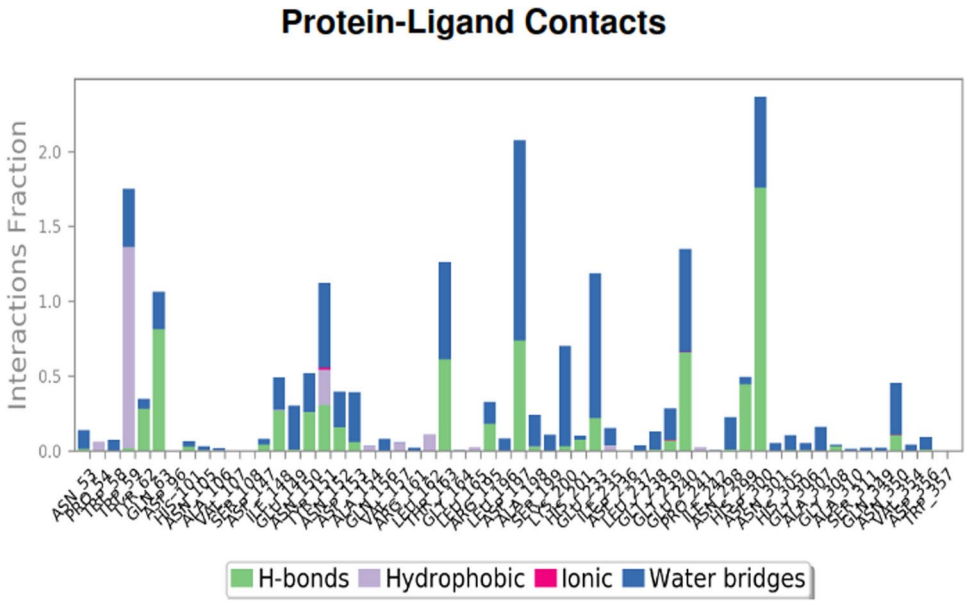


Fig. 12 Bar charts indicating the interactive contacts between Co–ligand and the amino acid residues of human pancreatic amylase

OCT2, and demonstrated higher negative BBB permeability (log BB), unlike the co-crystallized ligand with a log BB of (−4.265). None of the compounds acted as CYP2D6, CYP1A2, CYP2C19, or CYP2C9, CYP3A4 substrates or inhibitors, however, ZINC85490447 was a substrate of CYP3A4 (Table 2).

ZINC85593668 exhibits the highest total clearance value (1.015 log ml/min/kg) while the co-crystallized ligands showed negative clearance value. Only ranirestat showed potential AMES toxicity (Table 2). While none of the compounds were hERG I inhibitors, they were hERG II inhibitors. ZINC85593620 had the highest LD_{50} value (2.798 mol/kg). Acarbose had the highest maximum tolerated dose (0.435 log mg/kg/day), the co-crystallized ligands had (8.099 log mg/kg bw/day), while ranirestat had (1.552 log mg/kg bw/day) (Table 2). None of the compounds exhibit skin sensitization. Acarbose and co-crystallized ligands show significantly higher minnow toxicity values (16.823 and 20.95 log mM, respectively) while ZINC85593620 and ranirestat demonstrate lower minnow toxicity values (1.824 and 1.876 log mM, respectively). The natural compounds present varying toxicity potentials with ZINC85593620 and ZINC85490447 active for hepatotoxicity (Table 2).

Discussion

Molecular docking studies are pivotal in drug discovery as they predict the preferred orientation of a ligand when bound to a protein (Ibrahim et al. 2024b; Ugbe et al. 2023a). The

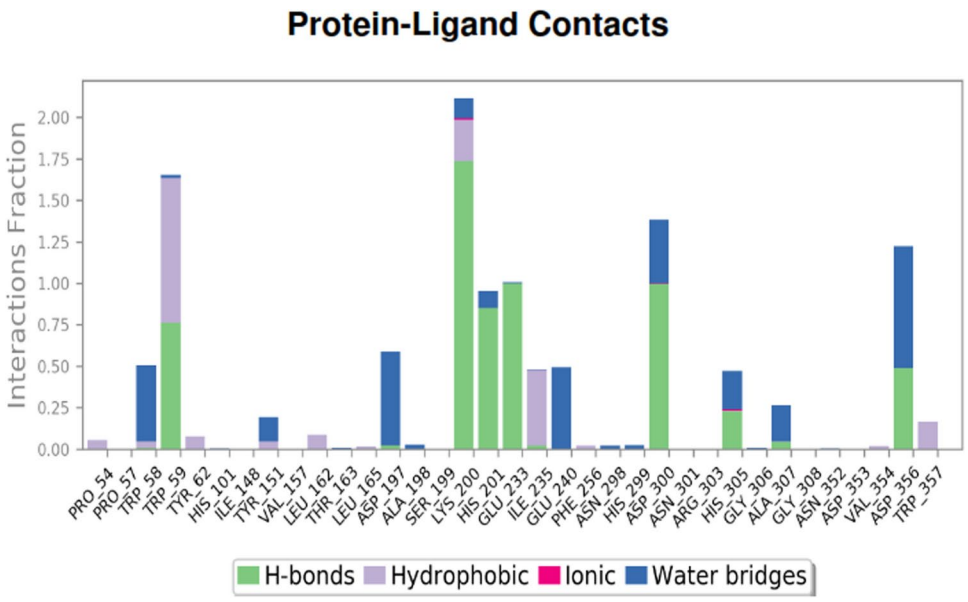


Fig. 13 Bar charts indicating the interactive contacts between ZINC85490447 and the amino acid residues of human pancreatic amylase

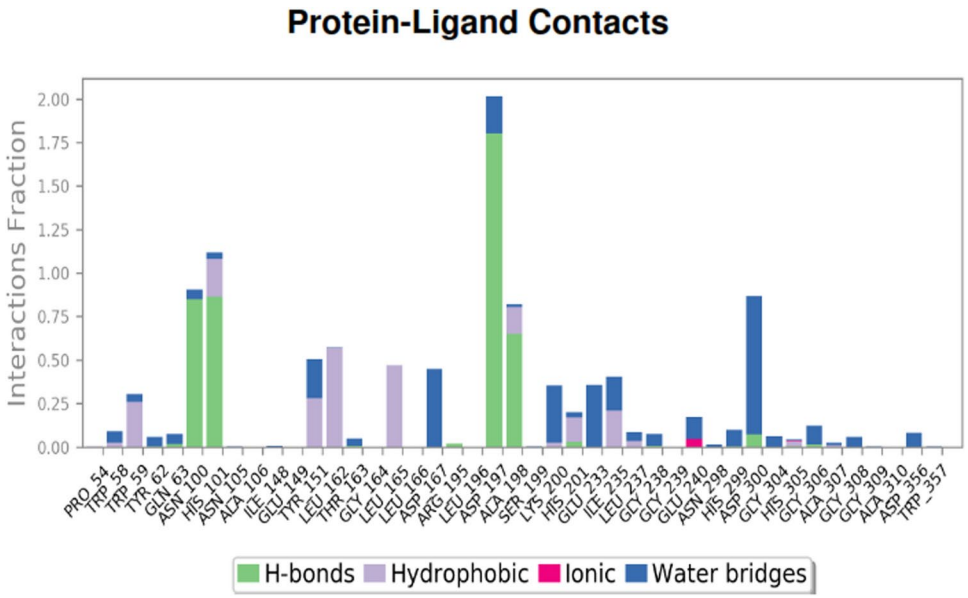


Fig. 14 Bar charts indicating the interactive contacts between ZINC85593620 and the amino acid residues of human pancreatic amylase

docking scores and binding energies provide key insights into the binding affinity and stability of the ligand-enzyme interactions (Alruhaimi et al. 2024; Alshammari 1456). The observed high docking score of ZINC85593620 indicates a strong binding pose of the compound with the enzyme and the interacting amino acid residues contributing to its stability within the binding pocket. The high docking scores and binding energies observed for compounds relative to the standards suggest their stronger binding pose and potential as inhibitors of the human pancreatic amylase enzyme. These compounds demonstrate robust interactions with critical residues, enhancing their orientation and binding affinity. This is in line with the study of Lukman et al. 2024a who reported that compounds with lower binding energies have better binding affinities. The comparative analysis with acarbose and ranirestat reinforces the efficacy of the ZINC compounds as promising therapeutic agents and better inhibitors of the human pancreatic amylase enzyme. This further provides a solid foundation for further experimental validation and drug development efforts (Rizk et al. 2024).

Validating the accuracy of molecular docking protocols is essential to ensure the reliability of predicted binding poses and interaction strengths (Bender et al. 2021). Superimposing the co-crystallized and re-docked ligands is a crucial step in this validation process, offering a direct comparison of predicted versus experimental conformations (Zhang et al. 2024; Ayipo et al. 2022). The RMSD value of 1.73 Å for is a crucial metric for assessing the accuracy of the docking protocol. Typically, an RMSD value of less than 2 Å is considered acceptable for validating docking accuracy

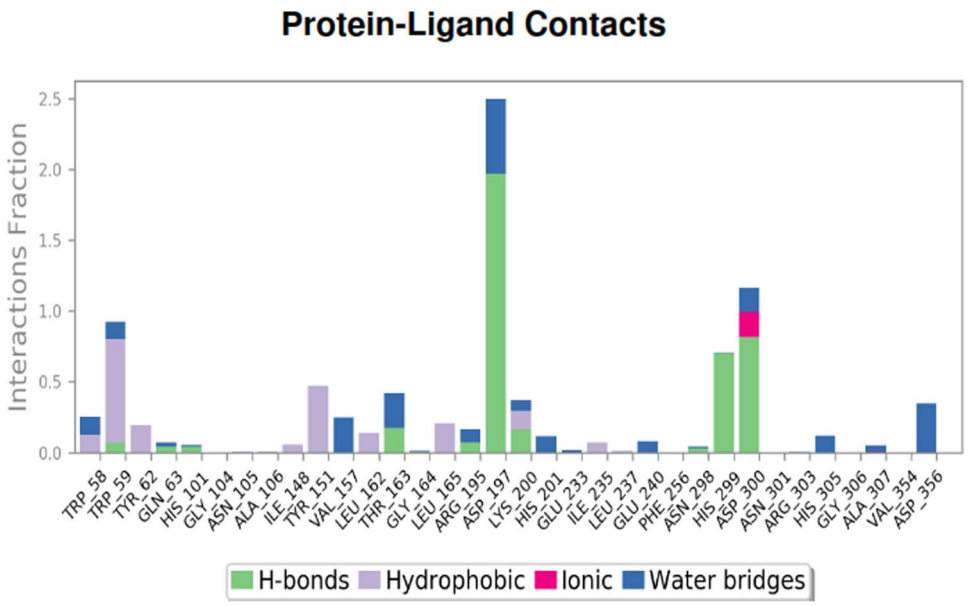


Fig. 15 Bar charts indicating the interactive contacts between ZINC85593668 and the amino acid residues of human pancreatic amylase

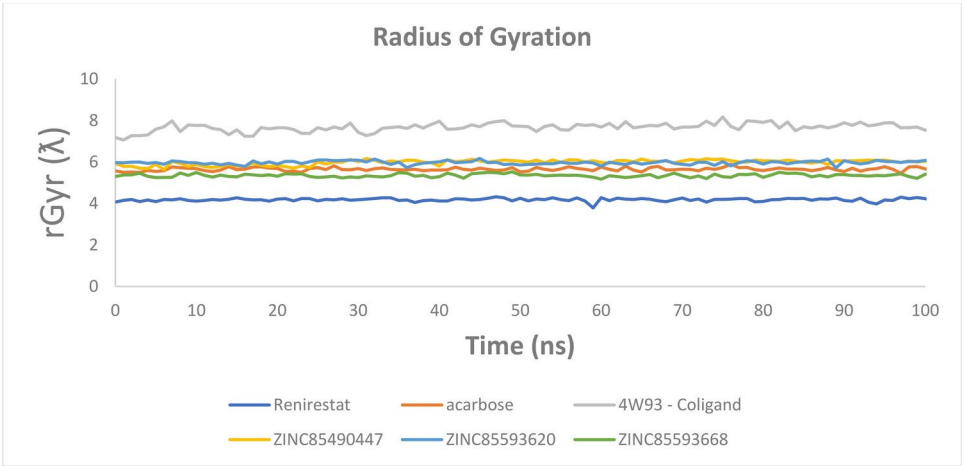


Fig. 16 Time-dependent rGyr during 100 ns MD simulations of human pancreatic amylase enzyme backbone with top ZINC compounds and reference drugs (acarbose and ranirestat)

(Golestanifar and Garkani-Nejad 2024). The low RMSD value observed here suggests a high level of agreement between the predicted and experimental conformations, thus affirming the reliability of the docking protocol. The close alignment of the docked and re-docked ligands indicates that the docking protocol accurately predicts the ligand's binding pose within the active site (Alshammari 1456). The observed ligand fitness within the active site, maintaining crucial interactions with key amino acid residues. This alignment suggests that the docking protocol effectively captures the essential binding interactions required for ligand efficacy. The validation of the docking protocol through superimposition and low RMSD values provides confidence in the subsequent docking studies. This ensures that the identified ligands are likely to exhibit similar binding poses and interactions in experimental conditions. The accurate prediction of ligand binding poses is fundamental for rationalizing new therapeutic agents and enhances the efficiency of drug discovery pipelines by reducing the need for extensive experimental validation at the initial stages (Saar et al. 2023).

Understanding the binding interactions between ligands and their target enzymes is crucial for rational drug design. The detailed analysis of 2D and 3D binding poses provides valuable insights into the specific interactions between the selected ligands and the human pancreatic amylase enzyme. The consistent hydrogen bonds and hydrophobic contacts observed across different ligands underscore the importance of these interactions in achieving stable and effective binding. Hydrogen bonds play a crucial role in stabilizing the ligand within the enzyme's active site (Wang et al. 2023). Residues such as GLU 233, ASP 300, and TRP 59 frequently engage in hydrogen bonding, contributing to the ligand's binding affinity. Hydrophobic contact interactions further stabilize the ligand–protein complex, ensuring that the ligand remains securely positioned within the active site.

Table 2 Predicted ADMET of the top ZINC compounds, co-crystallized ligands, and standards

Properties	ZINC85593620	ZINC85593668	ZINC85490447	4W93 Co-ligand	Acarbose	Ranirestat
Water solubility ((log mol/L))	−2.898	−2.886	−2.892	−2.892	−1.482	-2.91
CaCo2 permeability (log Papp in 10–6 cm/s)	−0.529	−0.421	−0.687	−0.975	−0.481	1.288
Intestinal absorption (human)(% Absorbed)	58.339	49.982	25.777	3.305	4.172	72.688
Skin Permeability (log Kp)	−2.735	−2.735	−2.735	−2.735	−2.735	−2.801
P-glycoprotein substrate	Yes	Yes	Yes	Yes	Yes	No
P-glycoprotein I inhibitor	No	No	No	No	No	No
P-glycoprotein II inhibitor	No	No	Yes	No	No	No
VDss (human) (log L/kg)	0.217	0.172	0.009	−0.104	−0.836	−0.68
Fraction unbound (human)	0.215	0.236	0.414	0.361	0.505	0.12
BBB permeability (log BB)	−2.454	−2.452	-1.558	−4.265	−1.717	−0.335
CNS permeability (log PS)	−4.389	−5.05	−3.582	−8.237	−6.438	−2.885
CYP2D6 substrate	No	No	No	No	No	No
CYP3A4 substrate	No	No	Yes	No	No	Yes
CYP1A2 inhibitor	No	No	No	No	No	No
CYP2C19 inhibitor	No	No	No	No	No	No
CYP2C9 inhibitor	No	No	No	No	No	No
CYP2D6 inhibitior	No	No	No	No	No	No
CYP3A4 inhibitior	No	No	No	No	No	No
Total Clearance ((log ml/min/kg))	0.619	1.015	0.124	−0.533	0.428	−0.123
Renal OCT2 substrate	No	No	No	No	No	No
AMES toxicity	No	No	No	No	No	Yes
Max. tolerated dose (human) (log mg/kg/day)	0.032	0.097	0.388	0.385	0.435	0.285
hERG I inhibitor	No	No	No	No	No	No
hERG II inhibitor	Yes	Yes	Yes	Yes	Yes	No
Oral Rat Acute Toxicity (LD50) (mol/kg)	2.798	2.637	2.483	2.482	2.449	2.125
Oral Rat Chronic Toxicity (LOAEL) (log mg/kg bw/day)	5.691	5.318	4.332	8.099	5.319	1.552
Hepatotoxicity	Yes	Yes	Yes	No	No	Yes
Skin Sensitization	No	No	No	No	No	No
T. Pyriformis toxicity (log ug/L)	0.285	0.285	0.285	0.285	0.285	0.299
Minnow toxicity (log mM)	1.824	2.27	9.279	20.95	16.823	1.876

Analysis of 2D and 3D binding poses highlights the critical interactions that contribute to the stability and efficacy of ligand binding to the target. These findings provide a robust foundation for the rational design of novel inhibitors, paving the way for further drug development efforts.

The MD simulation analysis is important to understand the binding stability of compound-target docked complexes (Ugbe et al. 2023b). RMSD is a critical metric used in MD simulations to analyze the stability of protein–ligand complexes. It measures the average deviation of the protein's backbone atoms from their initial positions over time (Jain et al. 2023), providing insights into the dynamic behavior and stability of the enzyme-ligand complexes (Jin and Wei 2024) This analysis focused on the RMSD of amylase backbone complexed with selected ligands and reference drugs, during a 100 ns MD simulation. The recorded slight fluctuation of ranirestat suggests a moderate stable interaction with the enzyme while acarbose complex indicated a stronger and more stable binding affinity with the enzyme. The high fluctuations in the co-ligand suggests that while the binding is generally stable, there are some conformational adjustments. However, ZINC85490447 demonstrated moderate fluctuations around 2.5 Å, suggesting some degree of flexibility but overall presented a stable binding while ZINC85593620 had a robust stability and minimal structural deviations. Similarly, ZINC85593668 formed stable and effective binding with minimal structural variations. The low and consistent RMSD values for most complexes, particularly acarbose and ZINC85593620, indicate strong and stable binding interactions. These ligands exhibit minimal structural deviations from their initial positions, suggesting effective inhibition of the enzyme. The comparative analysis of RMSD values among different ligands revealed that ZINC85593620 and ZINC85593668 demonstrated better stability than the standard reference drugs further highlighting their potential as robust enzyme inhibitors. The moderate fluctuations of ZINC85490447 maybe reflective of conformational flexibility, which can be advantageous for accommodating different binding pockets or dynamic environments. Ligands that maintain stable interactions

over prolonged simulation times are likely to exhibit higher efficacy and specificity in inhibiting enzymatic activity (Berselli et al. 2024). The consistent and low RMSD values of ZINC85593620 suggest strong and stable binding interactions, reinforcing their potential as effective enzyme inhibitors. This study underscores the importance of MD simulations in evaluating the dynamic behavior of protein–ligand complexes and guiding the rational design of novel therapeutic agents.

The RMSF measures the flexibility and stability of individual amino acid residues in a protein. By analyzing RMSF, we can gain insights into the dynamic behavior of the protein–ligand complex and identify regions of the protein that undergo significant conformational changes upon ligand binding (Hassan et al. 2023). The slight peaks observed in the RMSF values of acarbose and co-ligand bound complexes suggest regions of the protein that are more flexible. These flexible regions may play a role in accommodating ligand binding and facilitating enzyme activity. The RMSF values of ZINC85593620 and ZINC85593668 demonstrated comparable or even superior stability to reference drugs indicative of better potential as amylase inhibitors. The stability of the protein–ligand complexes, as indicated by the low RMSF values, is a key factor in the rational design of novel inhibitors. Ligands that maintain stable interactions over extended periods are likely to exhibit higher efficacy and specificity in inhibiting the enzyme's activity (Kamel et al. 2024).

The interactive contacts made by the complexes are critical for the stability and efficacy of the ligand binding within the enzyme's active site. The presence of ionic interactions and water bridges further stabilizes the complex while hydrophobic interactions and water bridges are prominent for high binding affinity and stability within the active site. However, moderate binding stability was observed in the standard-amylase complexes relative to the strong binding stability of the compounds. Hydrogen bonds are crucial for the specificity and strength of the ligand binding. ZINC85593620 and acarbose exhibit extensive hydrogen bonding, indicating strong and stable interactions within the active site. Hydrophobic interactions play a significant role in stabilizing the ligand–protein complex. The consistent hydrophobic contacts observed across different compounds highlight their importance in maintaining binding affinity. Ionic interactions and water bridges contribute to the overall stability of the protein–ligand complex (Chagaleti et al. 2024). The balanced distribution of these interactions in compounds suggests robust binding mechanisms in amylase inhibition. These findings provide a deeper understanding of the binding mechanisms and pave the way for the rational design of novel inhibitors with enhanced efficacy and stability.

The rGyr provides insight into the overall compactness and stability of protein–ligand complexes over time. It is useful in assessing conformational changes and structural stability during MD simulations (Swati et al. 2024). The consistent fluctuations of the standard references indicated stable compactness throughout the simulation period. The co-ligand complex shows minor fluctuations but remains largely stable, suggesting strong binding and minimal conformational changes. The observed minimal fluctuations in the ZINC compounds suggested a strong and stable interaction with the enzyme. The consistent and low fluctuations observed mostly in the natural compounds indicate strong binding interactions and minimal conformational changes. This stability is crucial for the effective inhibition of enzymatic activity (Cao et al. 2023). The minimal fluctuations observed in the rGyr for the co-ligand and the ZINC compounds relative to the standards further corroborate their potential as better and more effective inhibitors. Stable complexes are less likely to undergo significant structural changes that could diminish their binding affinity and inhibitory potential. Notably, the slight variations in the rGyr the natural compounds highlight the inherent flexibility and dynamic nature of protein–ligand interactions. However, the overall stability observed across all natural compound complexes indicates these ligands are promising candidates for further development as therapeutic agents. This is in line with the summation of Lukman et al. 2024b in their study.

In silico virtual screening such as ADMET profiling is crucial significant in evaluating the drug-likeness and potential pharmacokinetic profiles of compounds (Pradeepkiran et al. 2021). The solubility profile of the compounds is suggestive of their good solubility in physiological conditions. Compounds ZINC85593620 and ZINC85593668 with lower solubility and negative permeability values, indicating that formulation strategies may be necessary to improve their bioavailability such as solubilizing agents or nano-formulations, to improve their bioavailability (Patel et al. 2024). However, ZINC85593620 possessing better absorption probability than the other compounds, indicating good potential as an orally active drug.

The observed low skin permeability corroborates the potential of the compounds as oral drugs rather than for transdermal applications; the low absorption rate for acarbose and the co-ligand may limit their effectiveness when administered orally. The interaction of compounds with P-glycoprotein may impact the distribution and clearance of such compounds. Since the compounds are not P-glycoprotein I inhibitors, they might not significantly interfere with this efflux transporter, however, ZINC85490447, the only compound that acts as a P-glycoprotein II inhibitor, might not be significantly affected by absorption and distribution of drug efflux mechanisms. The recorded positive

VDss values of ZINC85593620 and ZINC85593668 indicate a relatively higher volume of distribution in the human body, which can enhance their therapeutic effect relative to acarbose and the co-ligand. With ZINC85593620 and ZINC85593668 exhibiting reasonable unbound fractions, although not up to acarbose suggest adequate availability for interaction with the target enzyme.

All the compounds are poorly penetrable into the central nervous system (CNS) based on the log BB and log PS values; this might reduce the risk of the compounds to cause CNS-related side effects. The compounds being non-inhibitors of the CYP450 enzymes and renal OCT2 substrates suggest a lower potential for drug-drug interactions. The positive VDss values and reasonable fraction unbound for ZINC85593620 and ZINC85593668 suggest they can achieve effective therapeutic concentrations in the body. There is higher probability of compounds especially ZINC85593668 to be cleared from the body relative to the standards and co-crystallized ligand. This reduces the potential of being toxic. While the compounds possess higher safety margin for human use, they also display a lower risk of cardiotoxicity relative to the standards and co-crystallized ligand. The high minnow toxicity values for acarbose and co-crystallized ligand indicate potential environmental risks, suggesting the need for environmental safety assessments and the exploration of more eco-friendly alternatives. Altogether, the natural compounds displayed better human pancreatic amylase inhibition and safety profile than the standards. However, further pre-clinical study is required to validate these findings.

Conclusion

In this study, the initial 24,316 ZINC compounds retrieved were screened to the top three; ZINC85490447, ZINC85593620, and ZINC85593668. The compounds demonstrated significant binding interactions and stabilities with amylase relative to the standards depicting their relevance for further development as antidiabetic drugs. While presenting remarkable ADMET properties, modifications might be required to enhance their solubility and hence greater efficiency. Thus, findings could serve as valuable guides for further development and optimization of these compounds as therapeutic agents. Further studies in vitro and in vivo studies could further validate the inhibitory effect of the compounds for potential development as antidiabetic drug candidates.

Authors contributions Conceptualization: [SOI]; Methodology: [YOA], Formal analysis and investigation: [SOI], Writing—original draft preparation: [SOI, YOA, HYL, FAA, AN, RAK, MFZ, OA]; Writing—review and editing: [SOI, YOA, HYL, FAA, AN, RAK, MFZ, OA], Supervision: [OA, MFZ].

Funding Authors received no funding for this work.

Data availability No datasets were generated or analysed during the current study.

Declarations

Conflict of interest The authors declare no competing interests.

References

Abdul Rasheed-Adeleke T, Lawal B, Agwupuye EI, Kuo Y, Ene AM, Ekoh OF, et al (2023) Apigetrin-enriched Pulmeria alba methanolic extract prevents assault of STZ on pancreatic β-cells and neuronal oxidative stress with concomitant attenuation of tissue damage and suppression of inflammation in the brain of diabetic rats.

Ahmed F, Samantasinghar A, Soomro AM, Kim S, Choi KH (2023) A systematic review of computational approaches to understand cancer biology for informed drug repurposing. J Biomed Inform 142:104373

Alruhaimi RS, Kamel EM, Alnasser SM, Alzoghaibi MA, Lamsabhi AM, Mahmoud AM (2024) Mechanistic insights into carbonic anhydrase IX inhibition by coumarins from *Calendula officinalis*: in vitro and in silico approaches. RSC Adv 14(45):33602–33618

Alshammari SO (2024) Computational insight of oleracone L, portulacatone B, and portulacatal from *Portulaca oleracea* L. as potential anticholinesterase inhibitors for Alzheimer's. Processes 12(7):1456

Arun N, Vettath RE (2024) Adverse events due to oral hypoglycemic drugs management of diabetic complications: calling for a team approach. Springer, Cham, pp 285–300

Asogwa FK, Ugwu CO, Ali JI (2023) Overview of diabetes and its curative approach using medicinal plants: a narrative review. GSC Adv Res Rev 15(1):130–143

Ayipo YO, Yahaya SN, Babamale HF, Ahmad I, Patel H, Mordi MN (2021) ß-Carboline alkaloids induce structural plasticity and inhibition of SARS-CoV-2 nsp3 macrodomain more potently than remdesivir metabolite GS-441524: computational approach. Turk J Biol 45(7):503–517

Ayipo YO, Alananzeh WA, Abdulsalam ZA, Badeggi UM, Jimoh AA, Osunniran WA et al (2022) Structure-based design and molecular simulations of some quercetin-based drugs as repurposable inhibitors of SARS-CoV-2 main protease. Trends Sci 19(21):2557

Ayipo YO, Alananzeh WA, Yahayaa SN, Mordi MN (2022) Molecular modelling and virtual screening to identify new piperazine derivatives as potent human 5-HT1A antagonists and reuptake inhibitors. Combin Chem High Throughput Screen

Bender BJ, Gahbauer S, Luttens A, Lyu J, Webb CM, Stein RM et al (2021) A practical guide to large-scale docking. Nat Protoc 16(10):4799–4832

Berselli A, Menziani MC, Muniz-Miranda F (2024) Structure and energetics of PET-hydrolyzing enzyme complexes: a systematic comparison from molecular dynamics simulations. J Chem Inf Model 64(21):8236–8257

Cao C, Yang N, Wang X, Shao J, Song X, Liang C et al (2023) Biomedicine meets nanozyme catalytic chemistry. Coord Chem Rev 491:215245

Chagaleti BK, Kumar BS, Rajagopal R, Alfarhan A, Arockiaraj J, Kumaradoss KM et al (2024) Targeting cyclin-dependent kinase 2 CDK2: insights from molecular docking and dynamics

simulation-a systematic computational approach to discover novel cancer therapeutics. Comput Biol Chem 112:108134
Edache EI, Uzairu A, Mamza PA, Shallangwa GA (2021) A mathematical modeling and molecular dynamic simulations in the investigation of novel type I diabetes treatment. Biomed J Sci Tech Res. 34(1):005509
Golestanifar F, Garkani-Nejad Z (2024) In silico design and ADMET evaluation of new inhibitors for PIM1 kinase using QSAR studies, molecular docking, and molecular dynamic simulation. Heliyon 10(19):e38309
Hassan MI, Umair M, Mathur Y, Mohammad T, Khan A, Sulaimani MN et al (2023) Molecular dynamics simulation to study thermal unfolding in proteins. Protein folding dynamics and stability: experimental and computational methods. Springer, Cham, pp 221–49
Hernandez HW, Soeung M, Zorn KM, Ashoura N, Mottin M, Andrade CH et al (2019) High throughput and computational repurposing for neglected diseases. Pharm Res 36:1–20
Hossain MJ, Al-Mamun M, Islam MR (2024) Diabetes mellitus, the fastest growing global public health concern: early detection should be focused. Health Sci Rep 7(3):e2004
Houglum JE, Harrelson GL, Seefeldt TM (2024) Drugs for treating diabetes mellitus. Principles of pharmacology for athletic trainers. Routledge, pp 268–289
Ibrahim SO, Lukman HY, Zubair MF, Amusan OT, Abdulkadri FR, Lawal B et al (2024a) An insight into the physicochemical, drug-likeness, pharmacokinetics and toxicity profile of *Kigelia africana* (Lam) bioactive compounds. Al-Bahir J Eng Pure Sci 4(1):4
Ibrahim SO, Lukman HY, Ebhohimen IE, Babamale HF, Abdulkadir FR, Hamid AA et al (2024b) Chemoinformatic-aided antidiabetic analysis of the therapeutic potential of phytoconstituents in eremomastax speciosa extracts. Borneo J Pharm 7(2):172–186
Jain P, Satija J, Sudandiradoss C (2023) Discovery of andrographolide hit analog as a potent cyclooxygenase-2 inhibitor through consensus MD-simulation, electrostatic potential energy simulation and ligand efficiency metrics. Sci Rep 13(1):8147
Jangid K, Devi B, Rani P, Kumar N, Kumar V, Kumar V (2024) Discovery of small-molecules as potential GSK-3β inhibitors for the treatment of Alzheimer's disease using pharmacophore-based virtual screening. ChemistrySelect 9(15):e202400808
Jin Z, Wei Z (2024) Molecular simulation for food protein–ligand interactions: a comprehensive review on principles, current applications, and emerging trends. Compreh Rev Food Sci Food Saf 23(1):e13280
Kamel EM, Alqhtani HA, Bin-Jumah M, Rudayni HA, El-Bassuony AA, Lamsabhi AM (2024) Deciphering molecular mechanisms underlying the inhibition of β-glucuronidase by xanthones from *Centaurium spicatum*. Bioorg Chem 150:107609
Khan M, Khan S, Alshammary FL, Zaidi S, Singh V, Ahmad I et al (2024) In silico analysis to identify potential antitubercular molecules in *Morus alba* through virtual screening and molecular dynamics simulations. J Biomol Struct Dyn 42(4):1924–1931
Khursheed R, Singh SK, Wadhwa S, Kapoor B, Gulati M, Kumar R et al (2019) Treatment strategies against diabetes: success so far and challenges ahead. Eur J Pharmacol 862:172625
Koufakis T, Mustafa O, Zebekakis P, Kotsa K (2020) Oral antidiabetes agents for the management of inpatient hyperglycaemia: so far, yet so close. Diabet Med 37(9):1418–1426
Lu X, Xie Q, Pan X, Zhang R, Zhang X, Peng G et al (2024) Type 2 diabetes mellitus in adults: pathogenesis, prevention and therapy. Signal Transduct Target Ther 9(1):262
Lukman HY, Kuo Y, Owolabi MS, Lawal B, Chen L-C, Ajenifujah OT et al (2024a) Evaluation of terpenes rich Hura crepitans extract on glucose regulation and diabetic complications in STZ-induced diabetic rats. Biomed Pharmacother 179:117308
Lukman H, Aribisala J, Akoonjee A, Sulyman A, Wudil A, Sabiu S (2024b) Modulation of dipeptidyl peptidase IV by Rooibos tea metabolites towards type 2 diabetes care: evidence from molecular dynamics simulation and density functional theory. Sci Afr 24:e02173
Lv Q, Chen G, He H, Yang Z, Zhao L, Zhang K et al (2023) TCMBank-the largest TCM database provides deep learning-based Chinese-Western medicine exclusion prediction. Signal Transduct Target Ther 8(1):127
Mahapatra R, Padhi RK, Chand S, Guru A, Mahapatra H, Khuntia M (2022) Direct and indirect cost of therapy in diabetes: the economic impact on the agricultural families in India. J Pharmaceut Negative Results 2022:4548–553
Mansuri R, Hirpara F, Dudhat K (2024) Diabetes mellitus: prevalence, knowledge and future consideration for the development of technological innovation. Anal Bioanal Electrochem 16(5):473–506
Olanrewaju OA, Sheeba F, Kumar A, Ahmad S, Blank N, Kumari R, et al. (2023) Novel therapies in diabetes: a comprehensive narrative review of GLP-1 receptor agonists, SGLT2 inhibitors, and beyond. Cureus 15(12).
Osmaniye D, Karaca Ş, Kurban B, Baysal M, Ahmad I, Patel H et al (2022) Design, synthesis, molecular docking and molecular dynamics studies of novel triazolothiadiazine derivatives containing furan or thiophene rings as anticancer agents. Bioorg Chem 122:105709
Patel D, Sethi N, Patel P, Shah S, Patel K (2024) Exploring the potential of P-glycoprotein inhibitors in the targeted delivery of anti-cancer drugs: a comprehensive review. Eur J Pharmaceut Biopharmaceut 198:114267
Pradeepkiran JA, Sainath S, Shrikanya K (2021) In silico validation and ADMET analysis for the best lead molecules. Elsevier, Brucella Melitensis, pp 133–176
Prajapati RN, Bhushan B, Singh K, Chopra H, Kumar S, Agrawal M et al (2024) Recent advances in pharmaceutical design: unleashing the potential of novel therapeutics. Curr Pharm Biotechnol 25(16):2060–2077
Rizk MN, Ketta HA, Shabana YM (2024) Discovery of novel Trichoderma-based bioactive compounds for controlling potato virus Y based on molecular docking and molecular dynamics simulation techniques. Chem Biol Technol Agric 11(1):110
Saar A, Ghahremanpour MM, Tirado-Rives J, Jorgensen WL (2023) Assessing metadynamics and docking for absolute binding free energy calculations using severe acute respiratory syndrome coronavirus 2 main protease inhibitors. J Chem Inf Model 63(22):7210–7218
Schönherr H, Ayaz P, Taylor AM, Casaletto JB, Touré BB, Moustakas DT et al (2024) Discovery of lirafugratinib (RLY-4008), a highly selective irreversible small-molecule inhibitor of FGFR2. Proc Natl Acad Sci 121(6):e2317756121
Stoica RA, Ștefan DS, Rizzo M, Suceveanu AI, Suceveanu AP, Serafinceanu C et al (2019) Metformin indications, dosage, adverse reactions, and contraindications. IntechOpen London, UK, Metformin
Sun H, Saeedi P, Karuranga S, Pinkepank M, Ogurtsova K, Duncan BB et al (2022) IDF Diabetes Atlas: Global, regional and country-level diabetes prevalence estimates for 2021 and projections for 2045. Diabetes Res Clin Pract 183:109119
Swati K, Varma SR, Parameswari R, Panda SP, Agrawal M, Prakash A et al (2024) Computational exploration of FOXM1 inhibitors for glioblastoma: an integrated virtual screening and molecular dynamics simulation study. J Biomol Struct Dyn. https://doi.org/10.1080/07391102.2024.2308772
Teo ZL, Tham Y-C, Yu M, Chee ML, Rim TH, Cheung N et al (2021) Global prevalence of diabetic retinopathy and projection of burden through 2045: systematic review and meta-analysis. Ophthalmology 128(11):1580–1591

Ugbe FA, Shallangwa GA, Adamu Uzairu IA (2023a) Combined QSAR modeling, molecular docking screening, and pharmacokinetics analyses for the design of novel 2, 6-diarylidene cyclohexanone analogs as potent anti-leishmanial agents. Progr Chem Biochem Res 6(1):11–30

Ugbe FA, Shallangwa GA, Uzairu A, Abdulkadir I (2023b) A 2-D QSAR modeling, molecular docking study and design of 2-arylbenzimidazole derivatives as novel leishmanial inhibitors: a molecular dynamics study. Advan J Chem Sect a 6(1):50–64

Wang C, Liu C, Zhu X, Peng Q, Ma Q (2023) Catalytic site flexibility facilitates the substrate and catalytic promiscuity of Vibrio dual lipase/transferase. Nat Commun 14(1):4795

Wang Y, Liu M, Jafari M, Tang J (2024) A critical assessment of traditional Chinese medicine databases as a source for drug discovery. Front Pharmacol 15:1303693

Weinberg Sibony R, Segev O, Dor S, Raz I (2023) Drug therapies for diabetes. Int J Mol Sci 24(24):17147

Yan Q, Li D, Jia S, Yang J, Ma J (2024) Novel gene-based therapeutic approaches for the management of hepatic complications in diabetes: reviewing recent advances. J Diabetes Complications. 38:108688

Zhang Z, Chen X, Lu P, Zhang J, Xu Y, He W et al (2017) Incretin-based agents in type 2 diabetic patients at cardiovascular risk: compare the effect of GLP-1 agonists and DPP-4 inhibitors on cardiovascular and pancreatic outcomes. Cardiovasc Diabetol 16:1–10

Zhang X, Shen C, Zhang H, Kang Y, Hsieh C-Y, Hou T (2024) Advancing ligand docking through deep learning: challenges and prospects in virtual screening. Acc Chem Res 57(10):1500–1509

Publisher's Note Springer Nature remains neutral with regard to jurisdictional claims in published maps and institutional affiliations.

Springer Nature or its licensor (e.g. a society or other partner) holds exclusive rights to this article under a publishing agreement with the author(s) or other rightsholder(s); author self-archiving of the accepted manuscript version of this article is solely governed by the terms of such publishing agreement and applicable law.